Electronic Supplementary Information (ESI)

Photocatalytic Activity of Ultrathin 2DPNs for Enzymatically Formic Acid Generation from $CO_2$and C-S/C-N Bonds Formation

Pooja Singh,[a] Rajesh K. Yadav,[a,*]ChandaniSingh,[a]Surabhi Chaubey,[a]Satyam Singh,[a]Atul P. Singh,[b] Jin-OoK Baeg,[e] Tae Wu Kim,[c,*] DzhardimalievaGulzhian[d]

[a]Department of Chemistry and Environmental Science, Madan Mohan Malaviya University of Technology, Gorakhpur, U.P. 273010, India. *Email: rajeshkr_yadav2003@yahoo.co.in

[b]Department of Chemistry, Chandigarh University, Mohali, Punjab, 140413, India.

[c]Department of Chemistry, Mokpo National University, Muan-gun, Jeollanam-do, 58554, Republic of korea. *Email: twkim@mokpo.ac.kr

[d]Institute of Problems of Chemical Physics of RAS, acad. Semenov av. 1,Chernogolovka, Moscow region, 142432, Russia.

[e]Korea Research Institute of Chemical Technology, Advanced Chemical Technology Division 100 Jang-Dong, Yusong Daejeon. KR 305-600.

Table of Content

1. General remarks

Propionic acid, benzaldehyde, pyrrole, chloroform, methanol, formatedehydrogenase, thiophenol, 2-mercaptopyridine, 2-amino-thiophenol, 4-chlorothiophenol,$NaH_2PO_4.2H_2O$, $Na_2HPO_4.2H_2O$, NAD^+, 4-bromomethylbenzonitrile, 1,4-dicyanobenzene, 4-aminobenzonitrile were purchased from sigma-aldrich. The organometallic mediator (Rh), [Cp*Rh(bpy)Cl]Cl, (Cp* = η_5-C_5Me_5, bpy = 2,2-bipyridyl) was synthesized by reported literature method.[1]

2. Instruments and measurements

UV-visible absorption spectra were recorded on Shimazu spectrophotometer. Fourier transform infrared (FT-IR) spectra were recorded on a Bruker ALPHA-T FT-IR spectrometer. Nano-zetasizer (NZS90) was used for the measurements of zeta-potential and particle size.Crystallinity and d-spacing were study byPowder X-ray diffractometer (Bruker, D8 Advance Eco). The molecularstructure of the 2-subsituted benzothiol compound was confirmed by ^1H NMR and ^{13}C NMR spectra.

3. Synthesis of 2DPNs photocatalyst

Step-I. Synthesis of 5,10,15,20-tetraphenyl- porphyrin (TPP)

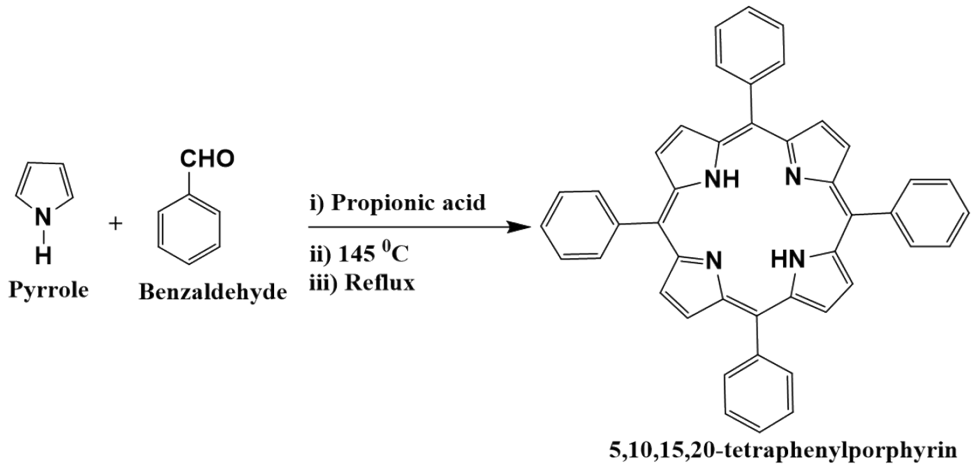

FigureS1: Synthesis of TPP monomer.

Step-II. Synthesis of 2DPNsphotocatalyst

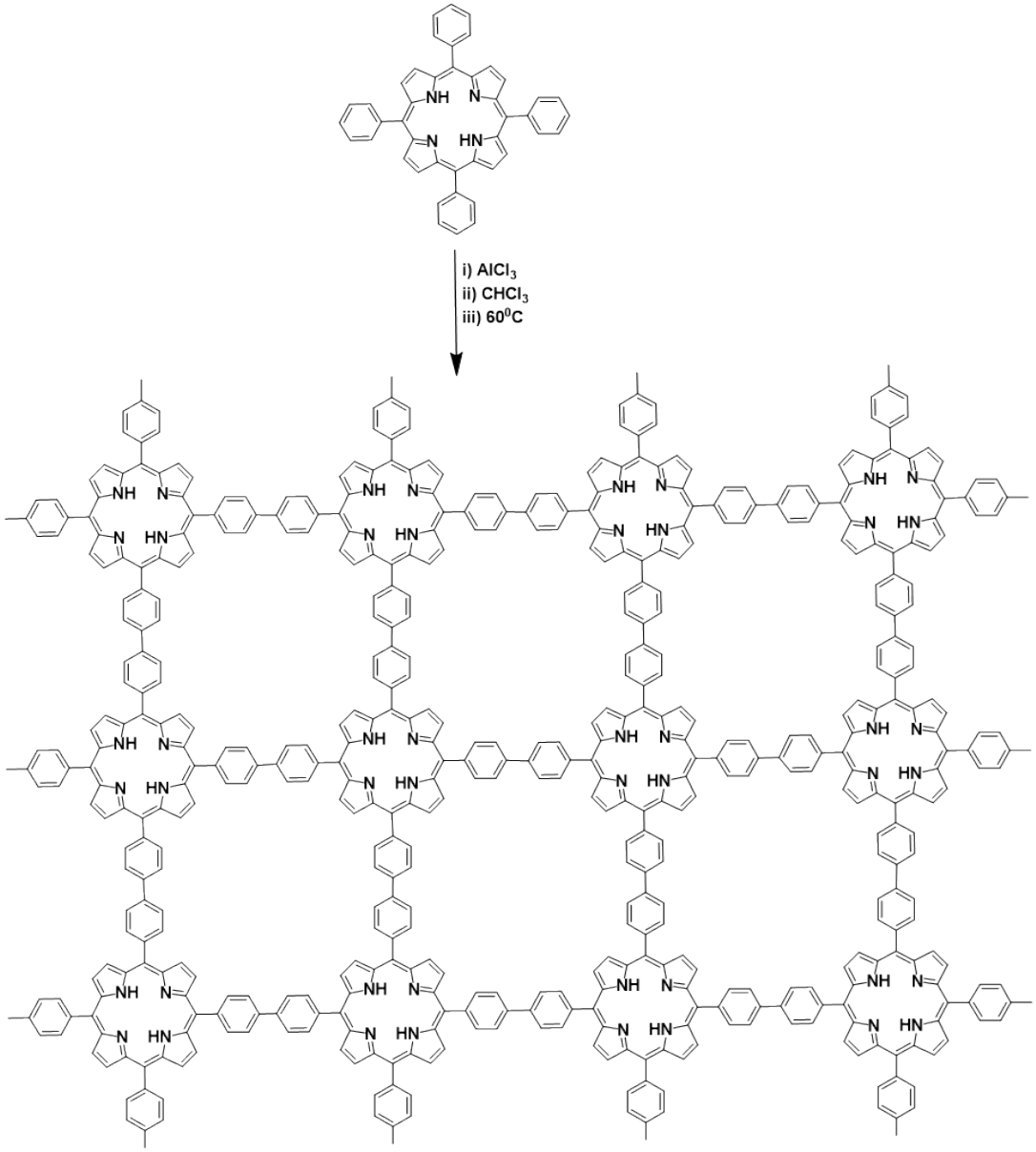

Figure S2: Synthesis of newly designed 2DPNsphotocatalyst for CO_2 to formic acid production and synthesisof 2-substituted BT.

4. Zeta potential analysis

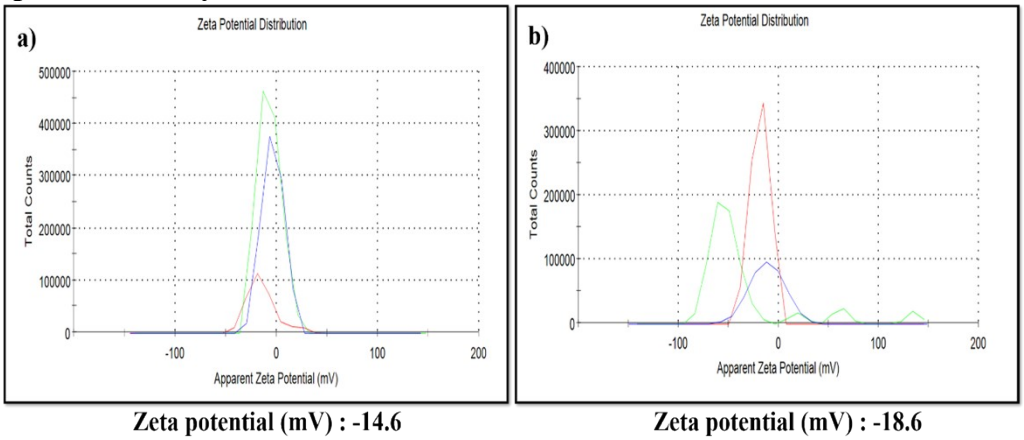

Figure S3. Zeta potential analysis of (a) TPP, and (b) 2DPNs photocatalysts.

5. Reusability test of 2DPNs photocatalyst for photocatalytic NADH regeneration and formic acid production:

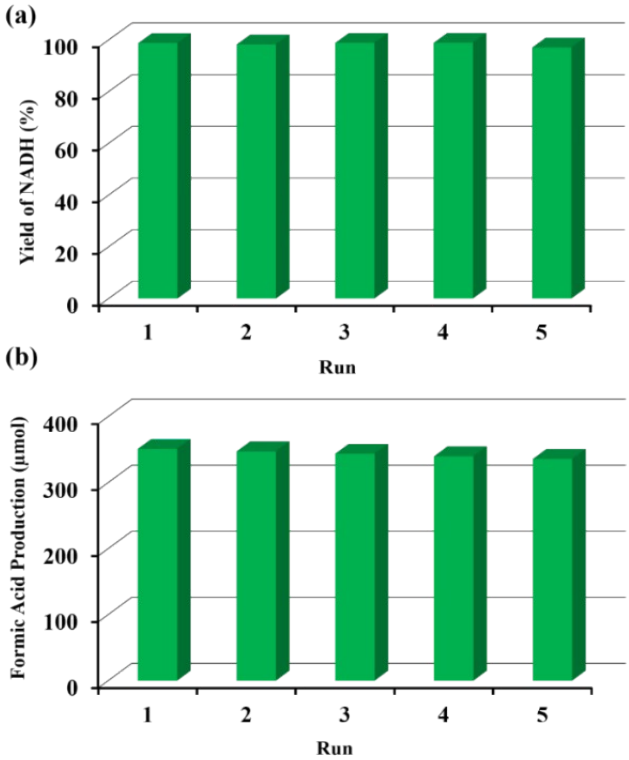

Figure S4. Reusability test of 2DPNs photocatalyst for (a) NADH regeneration, and (b) formic acid production up to fifth cycles. The photocatalysis was carried out using 2DPNs photocatalyst (2 mg) by illuminating the quartz reactor containing NAD^+ (248 µL), rhodium

complex (124 µL) andAsA(310 µL) in 3.1 mL of buffer solution (0.1M, pH~ 7.0). The formic acid production was performed in presence of format dehydrogenase (50 µL).

6. Reusability test of 2DPNs photocatalyst for synthesis of 2-substituted BT

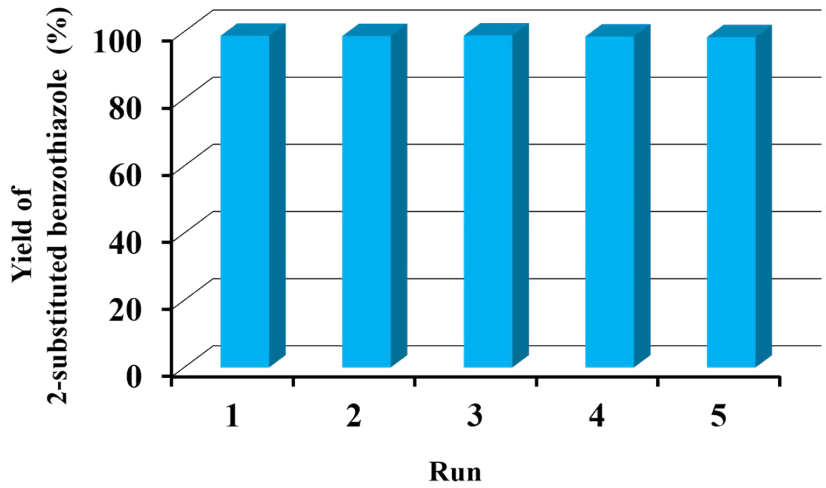

Figure S5: Reusability test of 2DPNs photocatalyst for synthesis of 2-substituted BT for 5 cycles. Reaction conditions: Tp (2eq.), N (1eq.), 2DPNs photocatalyst (5mg), DMSO (2 mL), 20 W blue LED lamps, rt, air,12 h.

7. Table S1: A Comparative reported literature survey for NADH regeneration and CO_2 to formic acid production.

Entry	Photocatalysts	Method	NADH regeneration (%)	Formic acid (μmol)	Time (h)	Fine chemical synthesis yield (%)	Ref.
1.	COF-367-Coll	Photochemical	.....	3.89	8	.....	2
2.	COF-367-Colll	Photochemical	.....	7.44	8	.....	2
3.	f-GQDs	Photochemical	74.95	198.96	2	.....	3
4.	ATCN-DSCN	Photochemical	74.02	290.4	9	.....	4
5.	$W_2Fe_4Ta_2O_{17}$	Photochemical	60.0	.....	14	.....	5
6.	CdTe Nanocrystals	Photochemical	55	.....	2	.....	6
7.	CdS Nanocrystals	Photochemical	53	.....	2	.....	6
8.	CdSe Nanocrystals	Photochemical	30	.....	2	.....	6
9.	NG-Co_3O_4-40	Electrochemical	.....	198.96	1	.....	7
10.	Ru/mpg-C_3N_4	Photochemical	.....	19.34	5	.....	8
11.	RuP/C3N4	Photochemical	.....	8.8	1	.....	9
12.	Fmoc-FF/g-C_3N_4	Photochemical	62.7	.....	3	.....	10
13.	$CaLa_4Ti_4O_{15}$	Electrochemical	.....	1.8	1	.....	11
14.	Hierarchical Cu pillar electrode	Electrochemical	.....	13.17	6	.....	12
15.	2D PNs	Photochemical	97.76	350.16	2	99.7	

8. Transmission electron microscopy (TEM)

To examine the morphology of the as-synthesized 2DPNs, we implemented the measurement using transmission electron microscopy (TEM). TEM images were collected by TECNAI G^2 F30 microscope (FEI company) operated at 300 keV. By using the same equipment, the high-resolution TEM images (HR-TEM) were collected. As shown in Figure S6a, the wide-view TEM image of 2DPNs powder shows the clear rectangular shapes with the sharp edges. The HR-TEM image shows the periodically aligned patterns around the edge of microcrystal, corresponding to the well-aligned layered structure. For the systematic characterization, we performed the fast Fourier transformation (FFT) of the ROI region indicated in Figure S6b. Based on the result from the FFT analysis, it can be learned that the spacing between the periodic lines is about 0.24 nm and the distance of 0.24 nm corresponds to the distance between the stacked 2D layers in the 2DPNs.

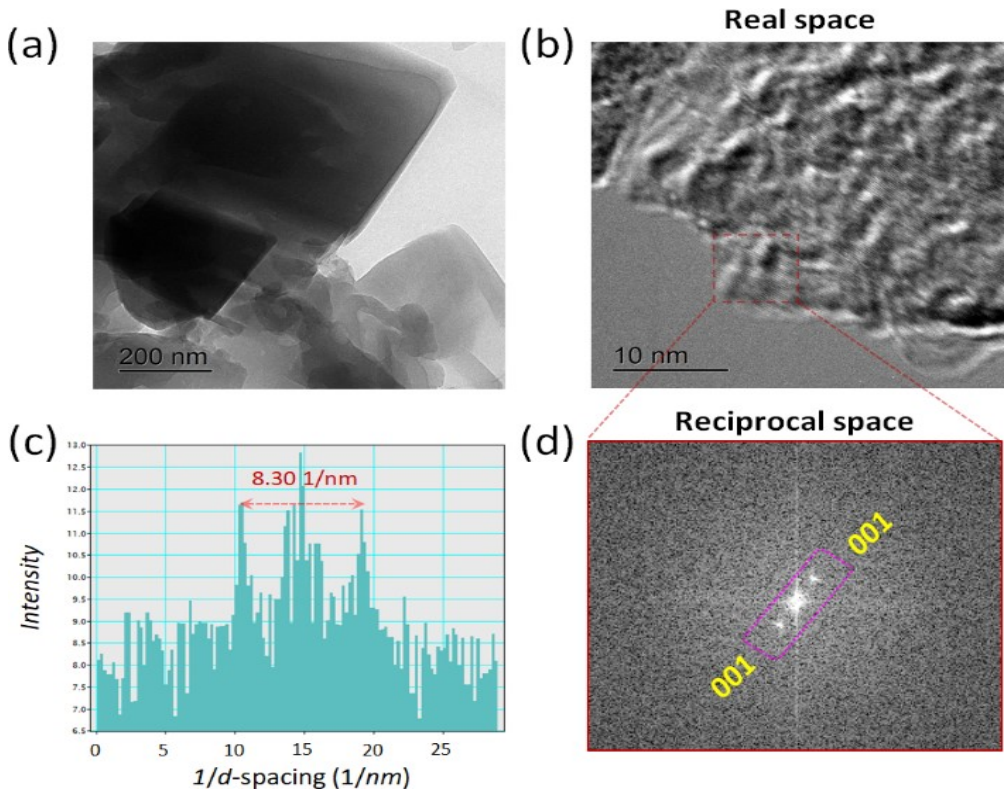

Figure S6. Transmission electron microscopy (TEM) measurement of 2DPNs. (a) TEM image of 2DPNs in powder form. (b) High-resolution TEM image. The region, indicated by the red dashed box, clearly shows the lattice patterns with several tens layers. (c, d) Results from the fast Fourier transformation (FFT) of the red dashed region in (b). (c) Profile plot of the area indicated by the magenta rectangle in (d). (d) Two-dimensional FFT image. The Bragg peaks for (001) planes with the spacing of 0.24 nm are seen. This value corresponds to the distance between the stacked 2D layers.

9. XRD analysis

To study the crystallinity and d-spacing value the as-synthesized 2DPNs photocatalyst, we performed the powder X-ray diffraction techniques. As depicted in Figure S7, the data from the measurement of powder X-ray diffraction (PXRD) of 2DPNs photocatalyst exhibited the XRD pattern around 21.5°, which refers to the interlayer stacking with the d-spacing of 0.4032 nm. In the small-angle region, the peak around 2.02^0 and $8.16^0$are attributed to the characteristic structure of 2D covalent organic frameworks.[13-14]

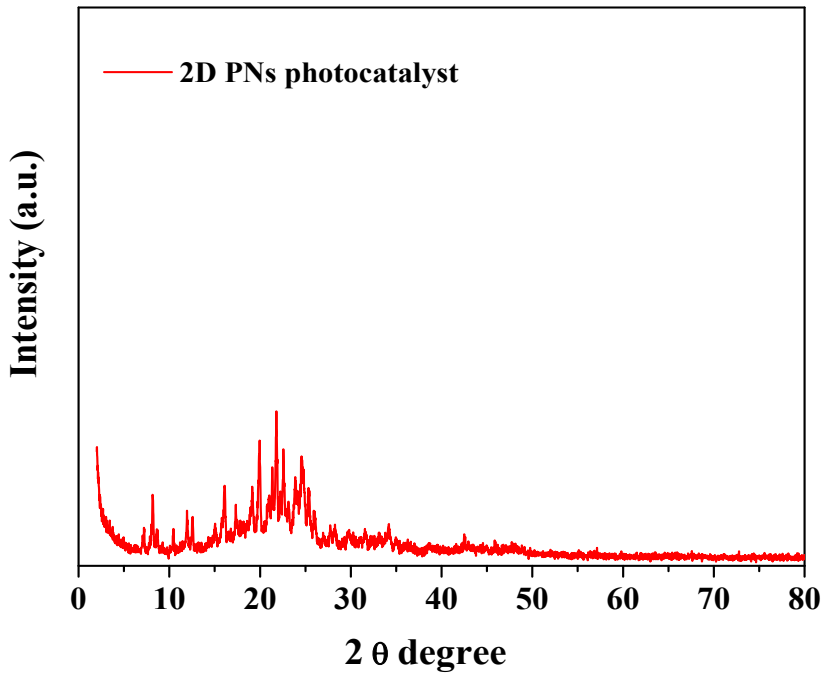

Figure S7: XRD analysis of 2D PNs photocatalyst.

10. Characterizations of 2DPNs photocatalyst after recycled experiment

To investigate the structures and stability of the 2DPNs photocatalyst after the photocatalytic reactions,we have characterised the 2DPNs photocatalyst afterward the recycled experiment through the XRD, FTIR and SEM analysis.As depicted in Figure S8, there is no difference exist in between two XRD (Figure S8a), FTIR (Figure S8b) and SEM analysis (FigureS8d), respectively.As a result, themolecular structure(XRD andFTIR analysis) and surface morphology (FigureS8d)of the 2DPNs photocatalyst wasremain same before and after the photocatalytic reactions (Figure S8a and S8b).

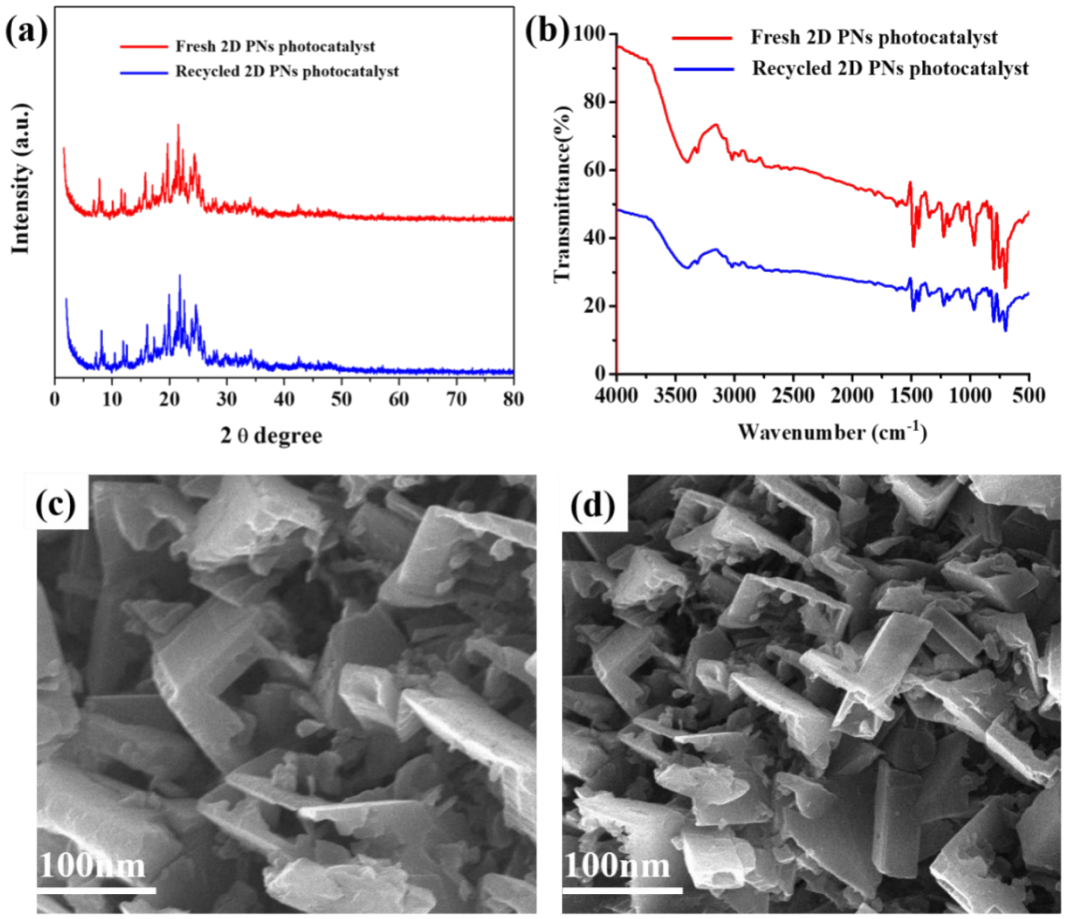

Figure S8: (a) XRD analysis of fresh and recycled 2DPNs photocatalyst (b) FTIR analysis of fresh and recycled 2DPNs photocatalyst (c) SEM analysis of fresh 2DPNs photocatalyst (d) SEM analysis of recycled 2DPNs photocatalyst.

11. HPLC (High performance liquid chromatography) experiment

We have performed the HPLC experiment to confirmed the formic acid (HCOOH) in the solution of 50% formic acid and methanol as shown in Figure S9a. We have also performed the HPLC experiment to confirmed the CO_2 conversion into formic acid (HCOOH)in the reaction mixture as shown in Figure S9b. [15]

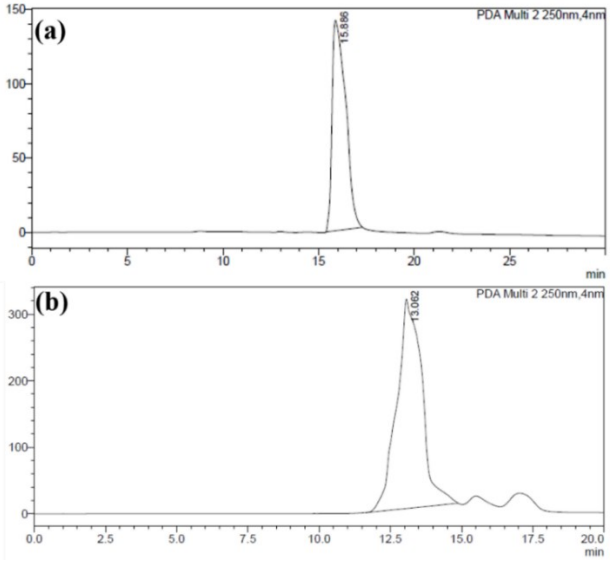

Figure S9. (a) Chromatogram of 50% formic acid solution in methanol (b) Chromatogram of formic acid (HCOOH) from CO_2solution (2DPNs photocatalyst (31 µL), NAD^+ (248 µL), rhodium complex (124 µL),AsA(310 µL) and format dehydrogenase enzyme (50 µL) in 3.1 mL of buffer solution).

12.Wavelength-dependent photocatalytic activity of the 2DPNs photocatalyst

As shown in Figure S10, the photocatalytic performance of the 2DPNs photocatalyst for CO_2 reduction is further studied by light irradiation of various wavelengths controlled by the specific long-press cut-off filters such as 420 nm, 450 nm, 500 nm, etc. The generation of formic acid correlates with the light-harvesting absorption spectrum of the 2DPNs photocatalyst as per the reported paper,[16-19] revealing that the CO_2 reduction reaction is a photocatalytic process.

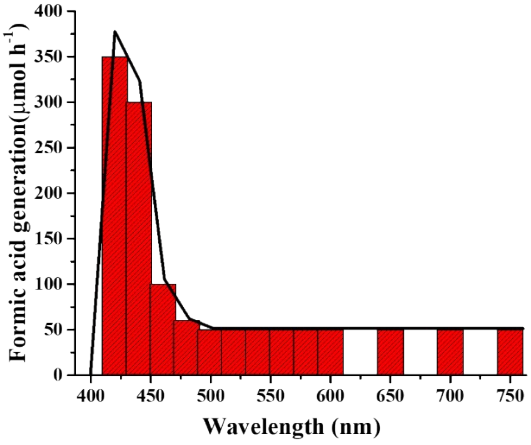

Figure.S10 Wavelength-dependent photocatalytic activity of the 2DPNs photocatalystfor CO_2 reduction reactions.

13. ^{1}H NMR and ^{13}C NMR spectra of 2-substiuted benzothiol compound

(i) ^{1}H NMR and ^{13}C NMR of 4-(thiazolo[5,4-b] pyridin-2-yl) aniline

^{1}H NMR ($CDCl_3$, 500 MHz): δ 8.43-8.10 (d, 1H), 7.65-7.63 (d, 1H), 7.59-7.57 (m,1H), 6.67-6.65 (s, 2H); ^{13}C NMR ($CDCl_3$, 500 MHz): δ 170.39, 148.86, 138.95, 133.81, 126.39.

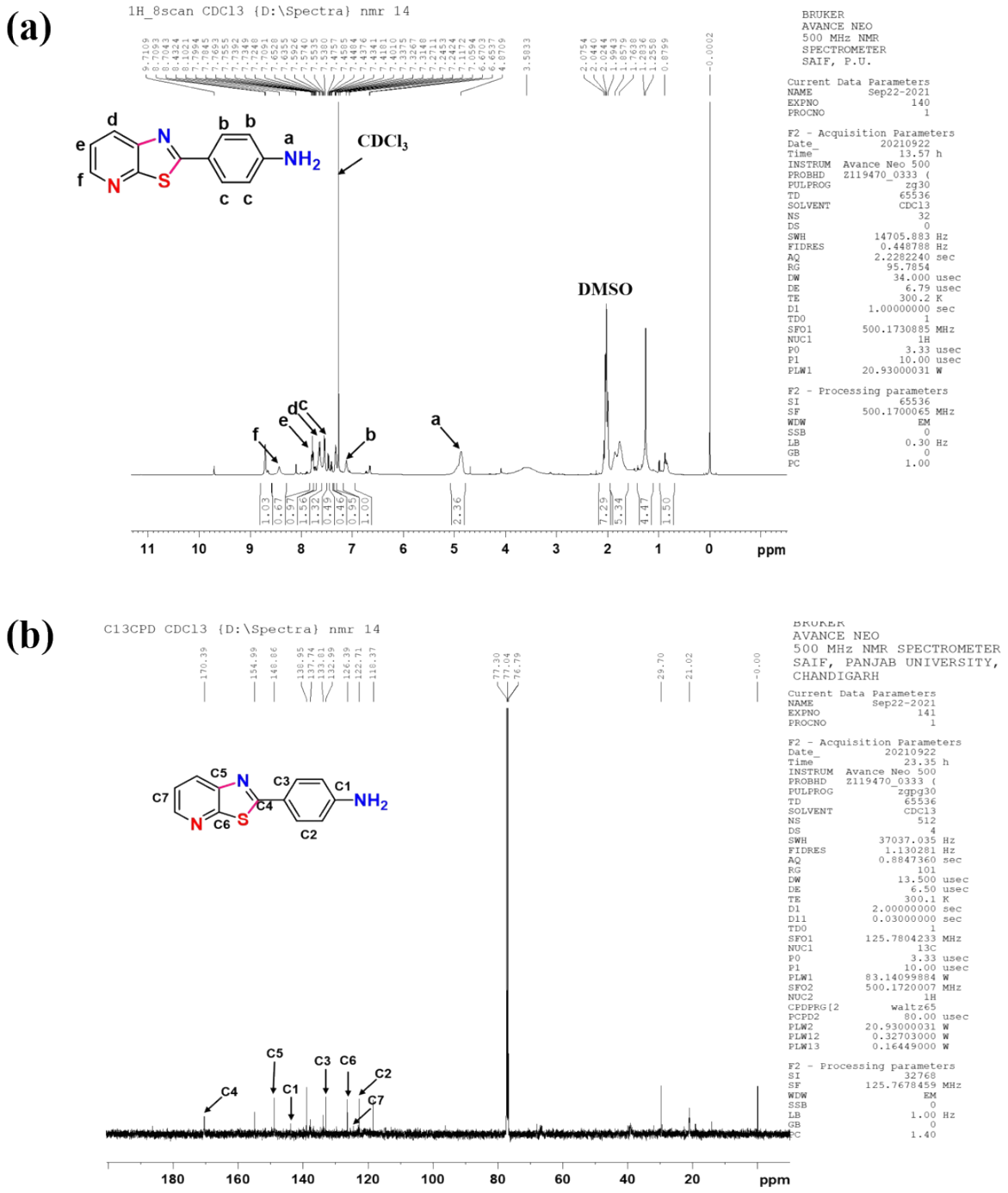

Figure S11. (a) ^{1}H NMR and (b)^{13}CNMR of 4-(thiazolo[5,4-b] pyridin-2-yl) aniline.

(ii)^{1}H NMR and ^{13}CNMR of 2-(4-(bromomethyl) phenyl) benzo[d]thiazol-7-amine

^{1}H NMR ($CDCl_3$, 500 MHz): 7.49-7.16 (d, 2H), 7.06-6.71 (d, 1H), 6.71-6.69 (d, 2H), 6.58-6.56 (s, 2H), 3.6 (s, 2H); ^{13}C NMR ($CDCl_3$, 500 MHz): δ 148.64, 133.29, 130.01, 118.20, 115.77, 38.66.

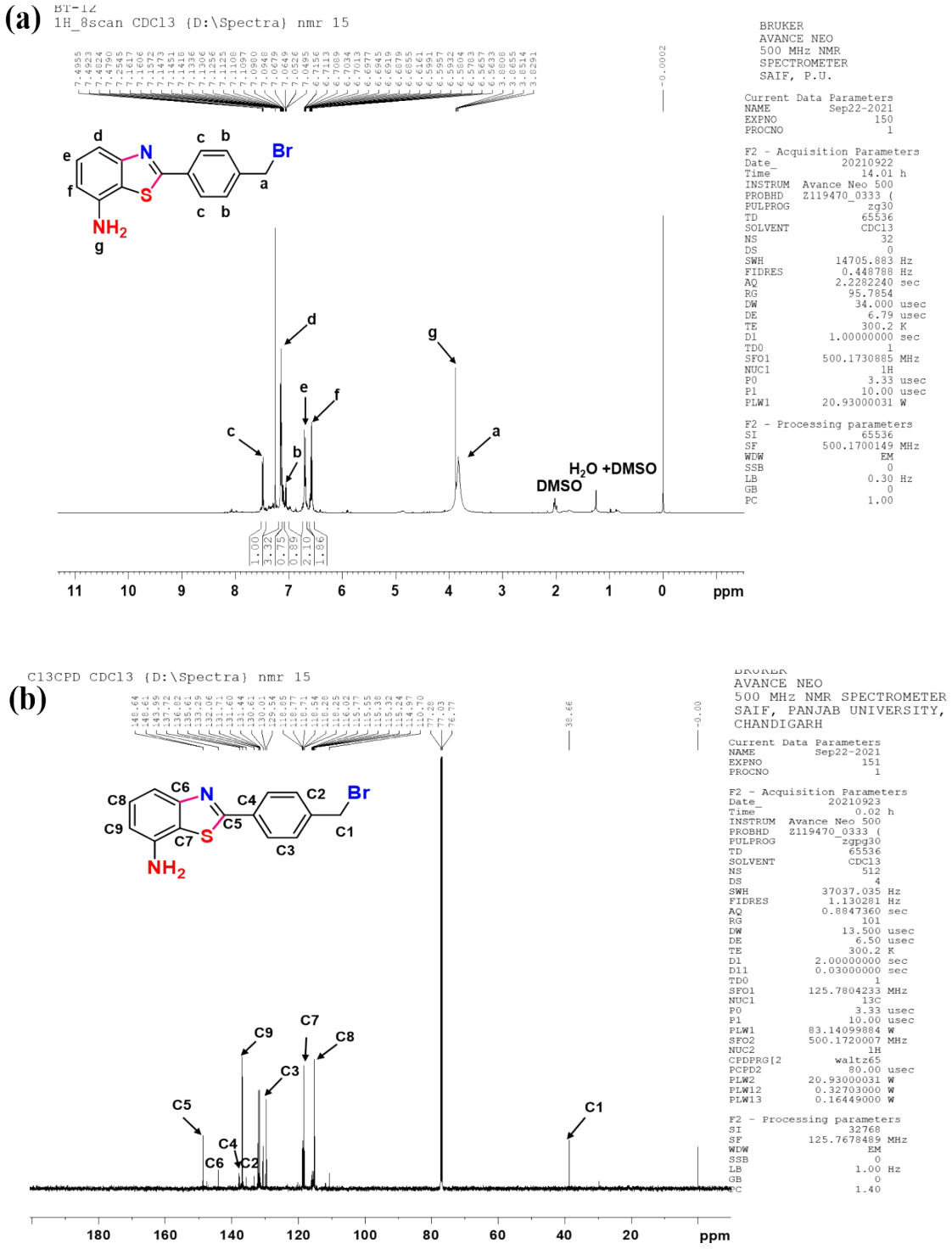

Figure S12.(a)^{1}H NMR and (b)^{13}CNMR of 2-(4-(bromomethyl) phenyl) benzo[d]thiazol-7-amine

(iii)^{1}H NMR and ^{13}CNMR of 2-(4-(bromomethyl) phenyl) thiazolo [5,4-b] pyridine:

^{1}H NMR ($CDCl_3$, 500 MHz): 8.19-8.17 (s, 1H), 7.77-7.75 (s, 1H), 7.48-7.47 (d, 2H), 4.47-4.40 (s, 2H); ^{13}C NMR ($CDCl_3$, 500 MHz): δ 167.48, 157.31, 144.36, 130.93, 124.93, 33.69.

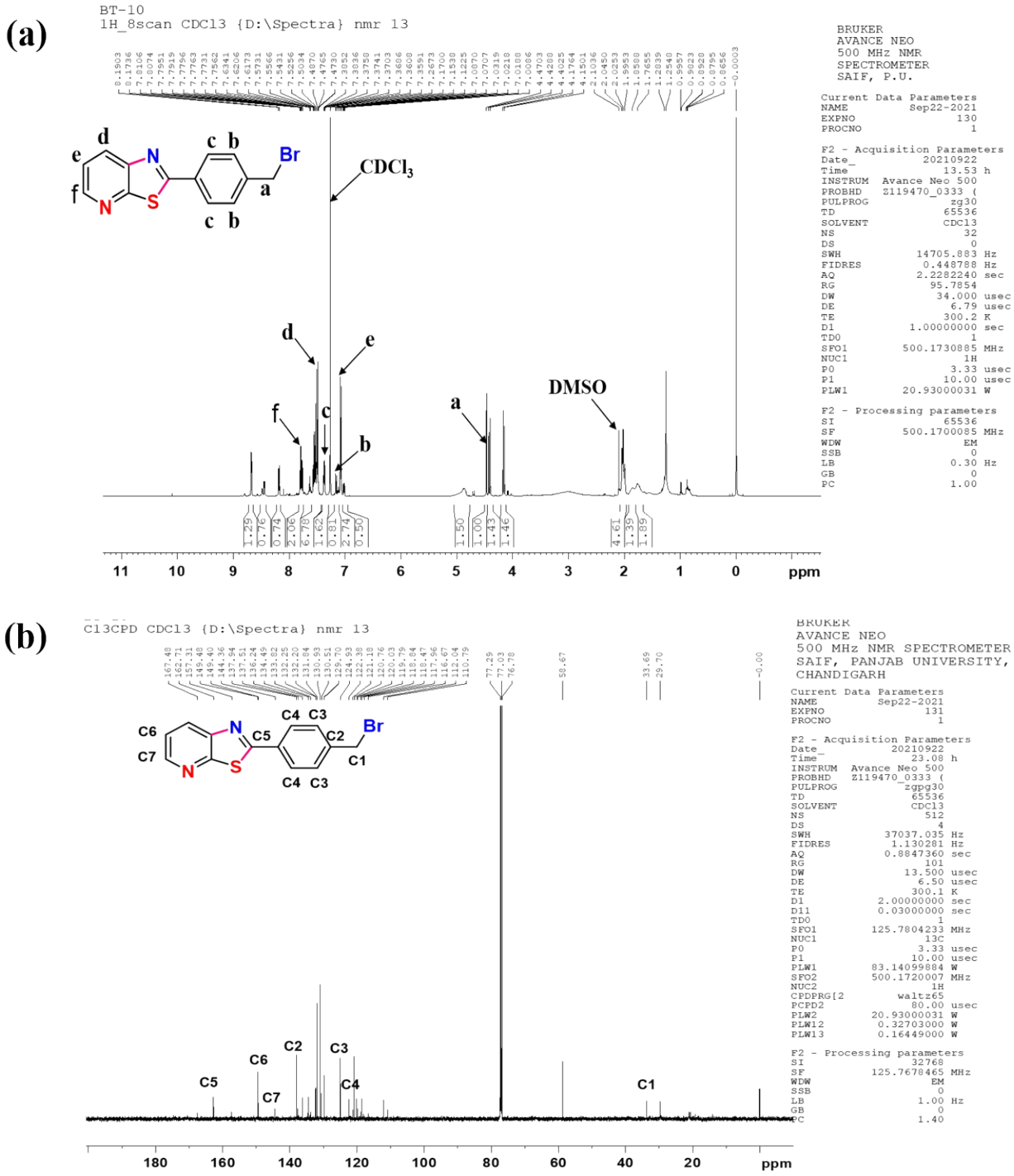

Figure S13.^{1}H NMR and ^{13}CNMR of 2-(4-(bromomethyl) phenyl) thiazolo[5,4-b] pyridine.

14. R_f value and image of synthesized 2-Substituted BT compounds

(i)

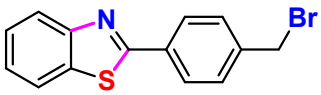

2-(4-(bromomethyl)phenyl)benzo[*d*]thiazole

R_f valueof starting material thiophenol = 0.82

R_f value of starting material 4-(bromomethyl benzonitrile) =0.83

R_f value of final product 2-(4-(bromomethyl) phenyl) benzo[d]thiazole = 0.89

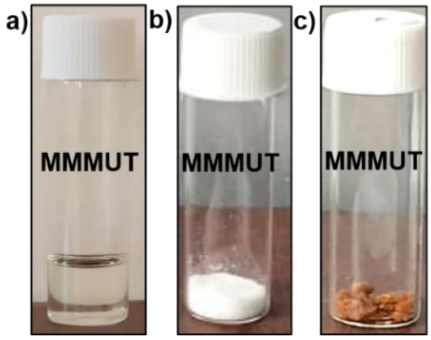

Figure S14. The sample image of (a) thiophenol (colourless liquid) (b) 4-(bromomethyl benzonitrile) (white crystal solid) (c) 2-Substituted BT (reddish brown solid).

(ii)

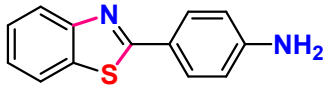

4-(benzo[*d*]thiazol-2-yl)aniline

R_f valueof starting material thiophenol = 0.82

R_f value of starting material 4-aminobenzonitrile =0.66

R_f value of final product 4-(benzo[d]thiazol-2-yl) aniline = 0.88

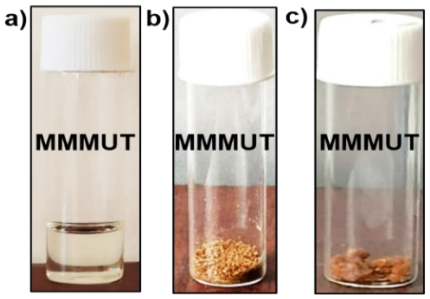

Figure S15. The image of (a) thiophenol (colourless liquid) (b)4-aminobenzonitrile (brown powder solid) (c) 4-(benzo[d]thiazol-2-yl) aniline (brown crystal solid).

(iii)

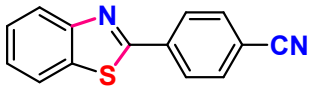

4-(benzo[*d*]thiazol-2-yl)benzonitrile

R_f valueof starting material thiophenol = 0.82

R_f value of starting material 1,4-dicyanobenzene=0.73

R_f value of final product 4-(benzo[d]thiazol-2-yl) benzonitrile = 0.75

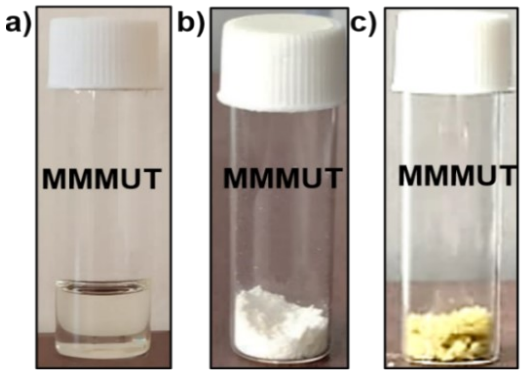

Figure S16. The image of (a) thiophenol (colourless liquid) (b) 1,4-dicyanobenzene (white solid) (c) 4-(benzo[d]thiazol-2-yl) benzonitrile (greenish solid).

(iv)

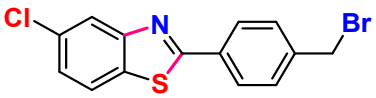

2-(4-(bromomethyl)phenyl)-5-chlorobenzo[*d*]thiazole

R_f valueof starting material 4-chlorothiophenol = 0.87

R_f value of starting material 4-(bromomethyl benzonitrile) =0.83

R_f value of final product 2-(4-(bromomethyl) phenyl)-5-chlorobenzo[d]thiazole = 0.89

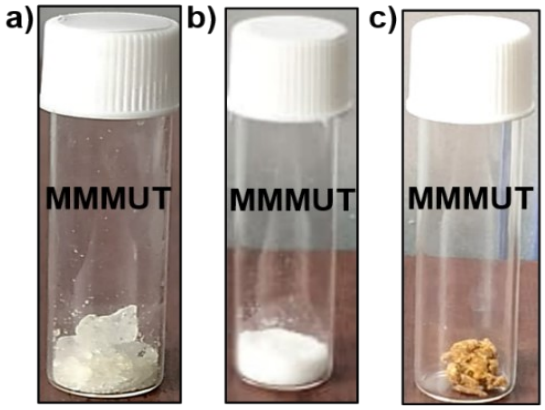

Figure S17. The image of (a) 4-chlorothiophenol (colorless solid) (b) 4-(bromomethyl benzonitrile) (white solid) (c) 2-(4-(bromomethyl) phenyl)-5-chlorobenzo[d]thiazole (brown solid).

(v)

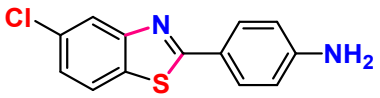

4-(5-chlorobenzo[*d*]thiazol-2-yl)aniline

R_f valueof starting material 4-chlorothiophenol = 0.87

R_f valueof 4-aminobenzonitrile = 0.66

R_f value of final product 4-(5-chlorobenzo[d]thiazol-2-yl) aniline = 0.68

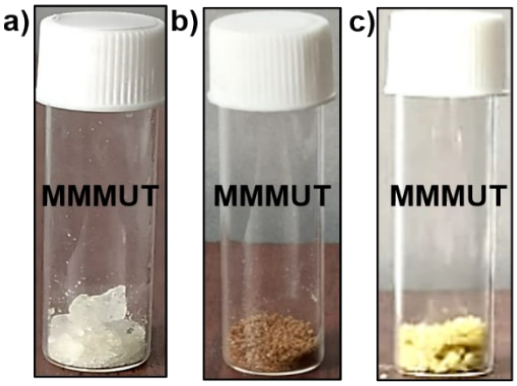

Figure S18. The image of (a) 4-chlorothiophenol (colourless solid) (b) 4-aminobenzonitrile (brown powder solid) (c) 4-(5-chlorobenzo[d]thiazol-2-yl) aniline (green solid).

(vi)

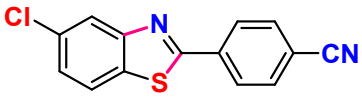

4-(5-chlorobenzo[*d*]thiazol-2-yl)benzonitrile

R_f valueof starting material 4-chlorothiophenol = 0.87

R_f valueof 1,4-dicyanobenzene = 0.73

R_f value of final product 4-(5-chlorobenzo[d]thiazol-2-yl) benzonitrile = 0.89

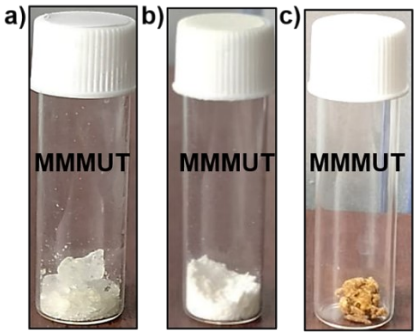

Figure S19. The image of (a) 4-chlorothiophenol (colourless solid) (b) 1,4-dicyanobenzene (white solid) (c) 4-(5-chlorobenzo[d]thiazol-2-yl) benzonitrile (brown solid).

(vii)

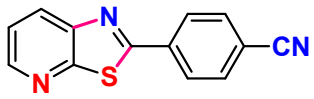

4-(thiazolo[5,4-*b*]pyridin-2-yl)benzonitrile

R_f valueof starting material 2-mercaptopyridine= 0.73

R_f valueof 1,4-dicyanobenzene = 0.73

R_f value of final product 4-(thiazolo[5,4-b] pyridin-2-yl) benzonitrile = 0.80

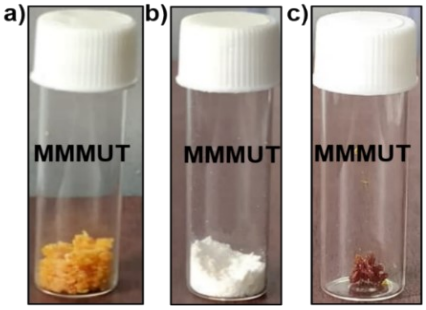

Figure S20. The image of (a) 2-mercaptopyridine (crystalline yellow solid) (b) 1,4-dicyanobenzene (white solid) (c) 4-(thiazolo[5,4-b] pyridin-2-yl) benzonitrile (crystalline reddish solid).

(viii)

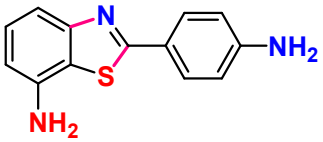

2-(4-aminophenyl)benzo[*d*]thiazol-7-amine

R_f valueof starting material 2-aminothiophenol(colourless oily solid) = 0.70

R_f valueof 4-aminobenzonitrile = 0.66

R_f value of final product 2-(4-aminophenyl) benzo[d]thiazol-7-amine = 0.83

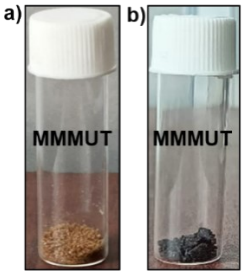

Figure S21. The image of (a) 4-aminobenzonitrile (brown powder solid) (b) 2-(4-aminophenyl) benzo[d]thiazol-7-amine (black solid).

(ix)

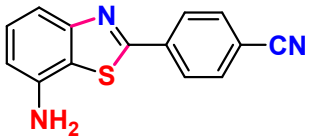

4-(7-aminobenzo[*d*]thiazol-2-yl)benzonitrile

R_f valueof starting material 2-aminothiophenol (colourless oily solid) = 0.70

R_f valueof 1,4-dicyanobenzene = 0.73

R_f value of final product 4-(7-aminobenzo[d]thiazol-2-yl) benzonitrile = 0.67

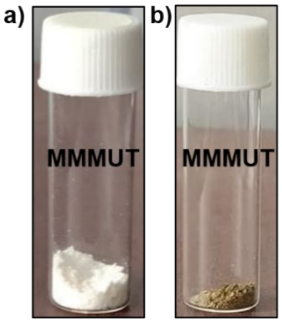

Figure S22. The image of (a) 1,4-dicyanobenzene (white solid) (b) 4-(7-aminobenzo[d]thiazol-2-yl) benzonitrile (grey solid).

15. References

1. S. H. Lee, D. H. Nam, J. H. Kim, J.-O. Baeg, C. B. Park, *Chem bio chem*2009, **10**(10), 1621-1624.
2. Y.-N. Gong, W. Zhong, Y. Li, Y. Qiu, L. Zheng, J. Jiang, H.-L. Jiang, *J. Am. Chem. Soc.* 2020, **142** (39), 16723–16731.
3. J. Meng, Y. Tian, C. Li, X. Lin, Z. Wang, L. Sun, Y. Zhou, J. Li, N. Yang,Y.Zong, F. Li, Y. Cao,H. Song, *Catal. Sci. Technol.***,** 2019**,9,** 1911-1921.
4. D. Yadav, R. K. Yadav, A. Kumar, N.-J. Park, J.-O. Baeg, *ChemcatChem,*2016,**8**(21), 3389–3393.
5. C. B. Park, S. H. Lee, E. Subramanian, B. B. Kale, S. M. Lee, J.-O. Baeg, *Chemical Communications*2008, (42), 5423.
6. D. H. Nam, S. H. Lee, C. B. Park, Small,2010, **6**(8), 922–926.
7. P. Sekar, L. Calvillo, C. Tubaro, M. Baron, A. Pokle, F. Carraro, A. Martucci, S. Agnoli, *ACS Catal.* 2017, **7**, 11, 7695–7703.
8. K. Maeda,K. Sekizawa, O. Ishitani, *Chemical Communications*2013, **49**(86), 10127.
9. R. Kuriki, K. Sekizawa, O. Ishitani, K. Maeda, *AngewandteChemie International Edition*, 2015 **54**(8), 2406–2409.
10. J. W. Ko, W. S. Choi, J. Kim, S. K. Kuk, S. H. Lee, C. B. Park, *Biomacromolecules* 2017, **18**(11), 3551–3556.
11. K. Iizuka, T. Wato, Y. Miseki, K. Saito, A. Kudo, *J. Am. Chem. Soc.* 2011, **133**(51), 20863–20868.
12. J.Chung, D. H. Won, J. Koh, E.-H. Kim, S. I. Woo, *Phys. Chem. Chem. Phys.***,**2016,**18**, 6252-6258.
13. A.P. Côté, H. M. El-Kaderi, H. Furukawa, J. R. Hunt, and O.M. Yaghi, *Journal of the American Chemical Society,* 2007, v. 129, 12914–12915.
14. K. Anjali, L. K. Nishana, J. Christopher, and A. Sakthivel, Journal of Porous Materials, 2020, v. 27, 1191–1201.
15. W. Zhao, Z. Wu, Z. Fan, S. Xiang, *Journal of Liquid Chromatography & Related Technologies, 41(9), 481–488.*
16. Y. Wang, S. Wang, X. W. Lou, *Angew. Chem. Int. Ed.* 2019, 58, **48**, 17236-17240.
17. B. Su, L. Huang, Z. Xiong, Y. Yang, Y. Hou, Z. Ding and S. Wang, *J. Mater. Chem. A***,**2019,**7**, 26877-26883.

18. Y. Ma, Y. Fang, X. Fu and X. Wang, *Sustainable Energy Fuels*, 2020,4, 5812-5817.
19. L. Huang, B. Li, B. Su, Z. Xiong, C. Zhang, Y. Hou, Z. Ding, S. Wang ,*J. Mater. Chem. A,*2020,**8**, 7177-7183.